Journal of Alloys and Compounds 509 (2011) 831–836

Contents lists available at ScienceDirect

Journal of Alloys and Compounds

journal homepage: www.elsevier.com/locate/jallcom

Structural characterizations of As–Se–Te glasses

G. Delaizir[a,*], M. Dussauze[b], V. Nazabal[c], P. Lecante[a], M. Dollé[a], P. Rozier[a], E.I. Kamitsos[b], P. Jovari[d], B. Bureau[c]

[a] Centre d'Elaboration de Matériaux et d'Etudes Structurales (CEMES-CNRS), 29 rue Jeanne Marvig, 31055 Toulouse, France
[b] Theoretical and Physical Chemistry Institute, National Hellenic Research Foundation, Athens, Greece
[c] Equipe "Verres et Céramiques", UMR CNRS 6226, Université de Rennes 1, 35042 Rennes, France
[d] Research Institute for Solid State Physics and Optics, H-1525 Budapest, POB 49, Hungary

ARTICLE INFO

Article history:
Received 10 July 2010
Received in revised form
10 September 2010
Accepted 18 September 2010
Available online 25 September 2010

Keywords:
Chalcogenide glass
Structure
NMR
WAXS
Raman

ABSTRACT

The atomic structure of chalcogenide glasses $As_3Se_{7-x}Te_x$ ($0 \le x \le 3$) and $As_2Se_{3-x}Te_x$ ($0 \le x \le 2.5$) has been investigated by different methods. Short-range order has been studied by Wide-Angle X-ray Scattering (WAXS). ^{77}Se NMR as well as Raman and infrared measurements were also performed on the different compositions. We show that the progressive introduction of tellurium in $As_3Se_{7-x}Te_x$ or $As_2Se_{3-x}Te_x$ induces breaking of Se–Se bonds and the formation of $AsSe_{3-x}Te_x$ pyramidal units. Experimental data also reveal the absence of Te–Te bonds even in the tellurium richest composition which let suppose a homogeneous repartition of tellurium atoms in the glassy network.

1. Introduction

Tellurium-based chalcogenide glasses are of growing interest because of their large transparency in the infrared range [1–3] that allow for example, CO_2 detection [4]. They are also very interesting for their thermo-mechanical or electrical properties [5,6].

In the case of the Te–As–Se ternary system, the special fiber composition $As_3Se_5Te_2$ is used as optical sensors to carry out Fiber Evanescent Wave Spectroscopy (FEWS) and investigate at molecular scale several problems encountered in microbiology, for example biochemical changes in human lung cells [7], or in environmental protection to monitor pollutants in waste water [8]. This glass is also widely used for space optics [9]. Despite these applications, there are only few papers dealing with the structure of the $As_3Se_5Te_2$ glassy network. Its knowledge is essential for a good understanding of mechanical, optical and chemical properties. An earlier study suggested a two-dimensional glass network of Se–Te–As chains, which are cross-linked by As–As bonds [10]. A recent study proposed a glass network structure built up of $As(Se,Te)_3$ pyramids in which twofold coordinated Te atoms substitute homogeneously twofold coordinated Se atoms [11].

In this paper, we aim to understand changes in the local glass structure as Te is added to the binary systems As_3Se_7 and As_2Se_3 to give glasses in the ternary systems $As_3Se_{7-x}Te_x$ ($0 \le x \le 3$) and $As_2Se_{3-x}Te_x$ ($0 \le x \le 2.5$). The techniques employed to probe chemical bonding and Se environments in these glasses are infrared, Raman and ^{77}Se NMR spectroscopy which are very powerful techniques and they have been already used to characterize structural chalcogenide glasses [12–14]. A radial distribution function (RDF) analysis was also performed on the Wide-Angle X-Ray Scattering (WAXS) measurement results, which are associated with the global average structural parameters.

2. Experimental

2.1. Sample preparation

Chalcogenide glasses in the As–Se–Te system were prepared by melting a batch of 10 g of appropriate amounts of commercially available tellurium (99.99%), arsenic (99.99%) and selenium (99.999%). The reactants were placed in an evacuated silica tube (10 mm in diameter) which was heated overnight in a rocking furnace at 650 °C. The ampoule was then quenched into water to obtain glass rods, which were subsequently annealed for 1 h near the glass transition temperature, Tg, to remove mechanical stresses induced on cooling. Then, the different samples were cooled to room temperature in few hours.

2.2. Measurements

2.2.1. ^{77}Se NMR spectroscopy

The ^{77}Se ($I = 1/2$) NMR spectra were recorded at room temperature on an Avance 300 Bruker spectrometer operating at 57.28 MHz with a 4 mm MAS probe spinning at 15 kHz. The spectra were recorded with the maximum spinning speed reachable (15 kHz), averaging simultaneously the chemical shift and reducing the homonuclear dipolar interaction between Se atoms. Fourier transformations were done on

* Corresponding author.
E-mail address: delaizir@icmpe.cnrs.fr (G. Delaizir).

0925-8388/$ – see front matter © 2010 Elsevier B.V. All rights reserved.
doi:10.1016/j.jallcom.2010.09.104

the entire magnetization to improve the signal to noise ratio and to avoid any distortion of the baseline. The processing and acquisition parameters were 3.5 μs π/2 pulse duration, 30 s recycle time, 1 MHz spectral width, time domain 1K, 3000 accumulated scans. The simulations of the experimental spectra were performed using a modified version of the Winfit Bruker Software.

2.2.2. Infrared and Raman spectroscopy

Infrared measurements were performed on As–Se–Te bulk glasses at room temperature on a Fourier-transform vacuum spectrometer (Bruker 113v), equipped with two sources (globar and Hg arc), two detectors (DTGS with KBr and polyethylene windows) and five different beam splitters, KBr for the mid-IR and four Mylar films for the far-IR (with thickness 3.5–25 μm), to cover the frequency range from 30 to 5000 cm^{-1}. Each spectrum results from the average of 400 scans measured with a typical resolution of 2 cm^{-1}. The infrared spectra of bulk glasses were recorded in the reflectance mode at quasi normal incidence (11°), and the complex refractive index of each sample was obtained through Kramers–Krönig analysis of its specular reflectance spectrum [15,16]. The infrared spectra reported in this work are in the form of absorption coefficient spectra, $\alpha(\nu)$, calculated from the relation $\alpha(\nu) = 4\pi\nu k(\nu) = 2\pi\nu\varepsilon''(\nu)/n(\nu)$, where $n(\nu)$ and $k(\nu)$ are the real and imaginary parts, respectively, of the complex refractive index, $\varepsilon''(\nu)$ is the imaginary part of the dielectric function and ν is the infrared frequency (in cm^{-1}).

Raman spectra were recorded at room temperature on a confocal micro-Raman instrument (Renishaw) in the backscattering geometry, using the 785 nm excitation line of a solid state laser with a typical resolution of 3 cm^{-1}. The spectrophotometer included a holographic Notch filter for Rayleigh rejection, a microscope equipped with a 100× objective and a CCD air cooled detector.

2.2.3. WAXS measurements

WAXS experiments were performed using a dedicated two-axis diffractometer. Measurements of the intensity scattered by the samples were performed at the molybdenum Kα (0.071069 nm) wavelength. The primary beam was graphite monochromatized, and fluorescence from As and Se was removed at measurement time by energy filtering of the solid state detector. Data sets typically included 457 measurements in the range $0° \le \theta \le 65°$ for equidistant s values [$s = 4\pi(\sin\theta/\lambda)$]. Bulk powder was introduced in thin walled Lindemann glass capillaries of 1.0 mm diameter. The same treatments were applied to all data sets, i.e. physical corrections for polarization and self-absorption as well as subtraction of the corrected scattering from glass capillary. A 400 μm $As_3Se_5Te_2$ fiber diameter was also used instead of the capillary to evaluate the effect of oxidation when crushing bulk glass into powder.

The so-called reduced intensity function was extracted and then Fourier transformed in order to obtain the RDF. A full description of this procedure can be found in [17]. Analysis of the experimental RDF provides good estimates of the mean atom–atom distances in the sample (d). The RDF is defined as the number of atoms at distance between r and $r+dr$ from the center of an arbitrary origin atom. It can be written as $D(r) = 4\pi r^2\rho(r)$ where $\rho(r)$ is the radial density function representing an atomic pair correlation function, and converging to the average density ρ_o for a large value of r. Below this limit, the $\rho(r)$ function exhibits peaks pointing to average interatomic separations. The position of the first peak in RDF gives the value of the average nearest-neighbor bond length r_1 and, similarly, the position of the second peak give the next nearest-neighbor distance r_2. Knowledge of both distances leads to the determination of the bond angle φ where $\varphi = 2\sin^{-1}(r_1/r_2)$ and, therefore, provides information about the different polyhedra constituting the network.

3. Results and discussion

3.1. ^{77}Se NMR results

^{77}Se 15 kHz MAS NMR spectra measured in this work are compared in Fig. 1 for four glass compositions As_3Se_7, As_4Se_6 (As_2Se_3), $As_3Se_5Te_2$ ($As_3Se_{7-x}Te_x$ with $x = 2$) and $As_4Se_4Te_2$ ($As_4Se_{6-x}Te_x$ with $x = 2$). The observed broadening of spectra is in accordance with the distribution of sites characterizing the amorphous state.

To understand the origin of As–Se–Te NMR spectra, the position of lines corresponding to the three expected type of sites of twofold coordinated Se are labeled by a, b and c in Fig. 1. Accordingly to [18], these lines are attributed to Se–Se–Se, Se–Se–As and As–Se–As sites, respectively. Indeed, the As_xSe_{1-x} glass network is built up of Se chains which cross-link $AsSe_3$ pyramids in agreement with the "chain crossing model" [18]. According to this model, As atoms are homogeneously distributed within the network and the length of Se chains cross-linking $AsSe_3$ pyramids depends on glass composition; the richer the composition in Se the longer the chains. In this classical frame, the network of As_2Se_3 (resp. $AsSe_3$) is constituted of $AsSe_3$ pyramids directly connected by Se corners (resp. Se–Se dimers) giving rise to a single c line (resp. b line) in the corresponding NMR spectrum [18]. The structure of As_3Se_7, that is to say $AsSe_{2.33}$, can be seen as intermediate between $AsSe_{1.5}$ (=As_2Se_3) and $AsSe_3$. We could therefore assume that As_3Se_7 is built up of corner sharing $AsSe_3$ pyramidal units cross-linked by either Se–Se bonds or direct bridging Se atoms. The related NMR spectrum does not fully agree with this simple model, since one needs to use simultaneously three Gaussian components to give an acceptable account of the experimental band shape (Fig. 2). In particular, the spectrum shows clearly that, even for this As-rich composition, Se–Se–Se short sequences are still present in the glass network [19,20]. Each band contribution has a Gaussian shape due to the structural disorder inherent to the glass, and the relative intensities of the three lines are in agreement with the initial stoichiometry.

The As_4Se_6 (As_2Se_3) and $As_4Se_4Te_2$ ^{77}Se NMR spectra are very similar (Fig. 1). No new lines or line shifts are observed. Thus, the introduction of tellurium in the initial composition does not modify significantly the selenium neighborhood in glass. This finding shows that Te substitutes preferentially Se than As in the glassy network. This is not surprising since Se and Te belong to the same family of the periodic chart and both are twofold coordinated.

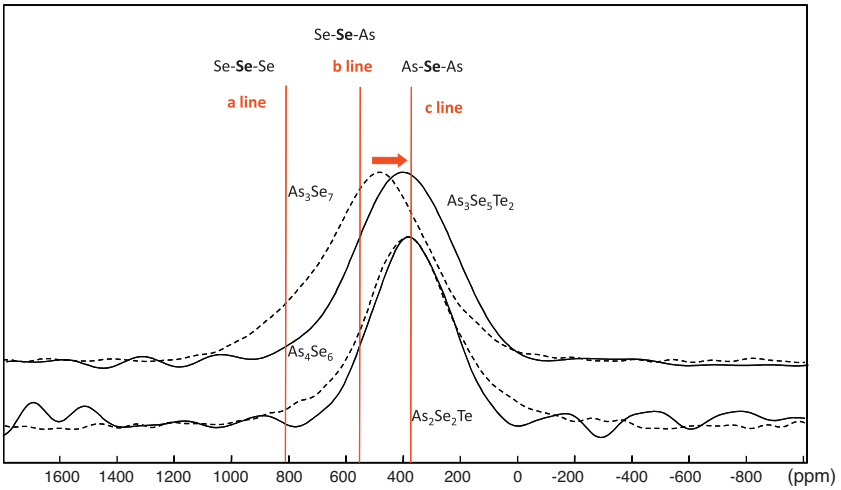

Fig. 1. Comparison of the ^{77}Se MAS NMR spectra of chalcogenide glasses in the As–Se–Te system with various Te contents. The arrow emphasizes the shift of the $As_3Se_5Te_2$ spectrum compared to that of As_3Se_7, while glasses $As_4Se_4Te_2$ and As_4Se_6 show similar spectra. The vertical straight lines indicate the position of the mean chemical shift associated with the three chemical bonding environments of Se in As_xSe_{1-x} glass [15].

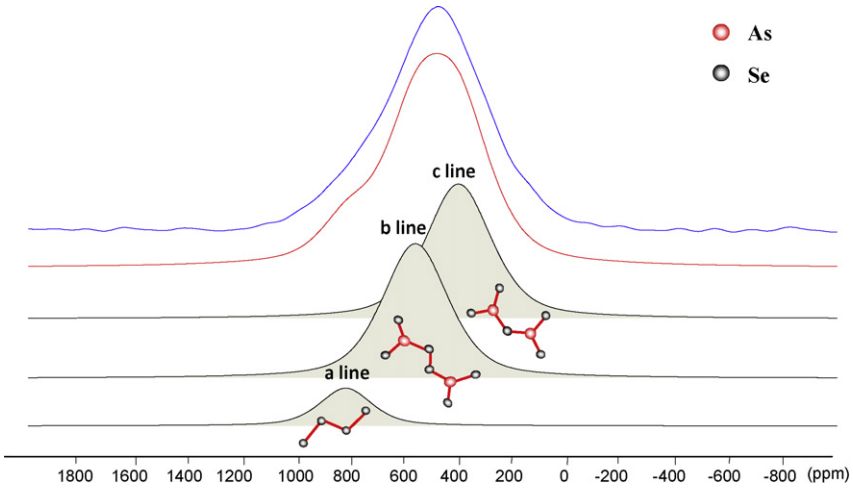

Fig. 2. ^{77}Se MAS NMR spectrum: reconstruction of the As_3Se_7 spectrum with three Gaussian bands assigned to sequences Se–Se–Se (a line 820 ppm), As–Se–Se (b line 560 ppm) and As–Se–As connecting the $AsSe_3$ pyramids (c line 380 ppm). The relative intensities (12%, 44% and 44%, respectively) are in agreement with the initial stoichiometry.

On the other hand, the introduction of tellurium in the As_3Se_7 glass, leading to $As_3Se_5Te_2$, modifies significantly the respective ^{77}Se NMR spectra (Fig. 1). While the a line (Se–Se–Se) contributes about 12% of the total As_3Se_7 band shape, its intensity vanishes totally in the $As_3Se_5Te_2$ spectrum. This observation demonstrates that the introduced tellurium tends to break Se–Se–Se sequences by substituting for Se atoms. Moreover, the general shift of the $As_3Se_5Te_2$ spectrum compared to that of As_3Se_7 is due also to tellurium. This is in agreement with previous observations [21] showing that the presence of tellurium in the first coordination shell of Se atoms induces the shift of the corresponding ^{77}Se NMR line toward lower chemical shift values. Thus, the shift of b line, assigned to As–Se–Se, indicates that part of the added tellurium substitutes Se atoms and leads to formation of As–Se–Te sites, in agreement with the chemical similarity of Te and Se atoms. On the other hand, the c line attributed to As–Se–As is still clearly visible and not shifted. Indeed, substitution of Se by Te in this kind of environment would have diminished this band, indicating that As–Te–As sites are not favored in these glasses. This is in good agreement with a previous study [11], where it was suggested that Te atoms are homogeneously dispersed in the $As_3Se_5Te_2$ glassy network.

3.2. Infrared and Raman results

Figs. 3 and 4 present Raman and IR spectra of bulk glasses in the systems $As_2Se_{3-x}Te_x$ and $As_3Se_{7-x}Te_x$ from $x = 0$ to $x = 2.5$ and 2, respectively. As shown by NMR [18], the As_2Se_3 bulk glass can be described as having a network constituted mainly of $[AsSe_{3/2}]$ trigonal pyramidal units connected by their corners. The IR bands at 230 and 110 cm^{-1} are assigned to characteristic modes of $[AsSe_{3/2}]$ pyramids, i.e. to their asymmetric stretching (υ_3) and bending (υ_2) modes, respectively, while the symmetric stretching (υ_1) vibration of $[AsSe_{3/2}]$ pyramids gives rise to the strong Raman band at 225 cm^{-1} [22,23]. Besides these features associated with $AsSe_{3/2}$ pyramids, the infrared and Raman spectra of As_2Se_3 glass show also activity above 250 cm^{-1} which indicates the presence of additional structural units.

For the bulk As_3Se_7 composition, the glass network is composed mainly of corner sharing $[AsSe_{3/2}]$ pyramids and $[AsSe_{3/2}]$ pyramids connected by Se–Se bonds as described above. Indeed, for the As_3Se_7 glass the excess of Se would lead to the formation of –Se–Se– bonding in various arrangements including As–Se–Se–As bridges and Se_n chains. The main mode associated with Se_n chains is expected at 238 cm^{-1} in the Raman spectrum [23–27], and this might be part of the broad band observed from 200 to 280 cm^{-1} for As_3Se_7 glass. Also, a Raman contribution of As–Se–Se–As entities is expected at ca. 270 cm^{-1} [26]. It should be noted that the high frequency IR shoulder at ca. 260 cm^{-1} and the corresponding Raman feature at ca. 250 cm^{-1} are generally related to Se_8 rings [23–27]. This finding is also in good agreement with the NMR spectrum which exhibits a signal above 800 ppm related to such sequences.

Upon substituting Se by Te, the high frequency components in the 250–270 cm^{-1} range loose gradually intensity in both Raman and IR spectra (Figs. 3 and 4), a result demonstrating the gradual destruction of Se–Se bridges in the two series of glasses. In the Raman spectrum, two intense bands develop at 168 and 205 cm^{-1} and become the main features at $x = 2.5$ for $As_2Se_{3-x}Te_x$ ($x = 2$ for $As_3Se_{7-x}Te_x$) glasses. The Raman band at 205 cm^{-1} can be attributed to vibrations of Se–Te bonds, as observed in the system $Se_{1-x}Te_x$ [28], or to As–Se vibration in mixed $AsSe_{3-x}Te_x$ units [29,30]. The latter proposition may contribute predominantly to this Raman band. The As–Te stretching in tellurium rich $AsSe_{3-x}Te_x$ entities ($x \geq 2$) would give rise to the Raman band at 168 cm^{-1} [29,30]. The presence of Te–Te bonds are not expected from Raman analysis of the spectra which should have a signature at 150–155 cm^{-1} [28]. The IR spectra of the $x = 2$ and $x = 2.5$ glasses shows their main band at 220 cm^{-1}. This is consistent with the formation of mixed $AsSe_{3-x}Te_x$ units, since the υ_3 mode of $[AsSe_{3/2}]$ pyramids is active at 230 cm^{-1} (Fig. 4).

To summarize, the progressive introduction of tellurium in the structure of glasses $As_3Se_{7-x}Te_x$ and $As_2Se_{3-x}Te_x$ induces the breaking of Se–Se bonds and the formation of Te–Se bonds and $AsSe_{3-x}Te_x$ pyramidal units, in good agreement with ^{77}Se NMR results.

3.3. WAXS results

The covalent radii of Te, As and Se atoms are, respectively, 0.138, 0.119 and 0.12 nm. Thus, small peaks appearing at very short distances in Figs. 5 and 6 (e.g. 0.08 nm) are clearly of spurious origin, since no distance smaller than the sum of the smallest atomic radii involved in the glass composition can occur.

The peak observed at $r = 0.17$ nm is due to superficial oxidation (Se–O or As–O) occurring when the bulk glass is crushed into powder. To make sure that this oxidation does not affect the overall

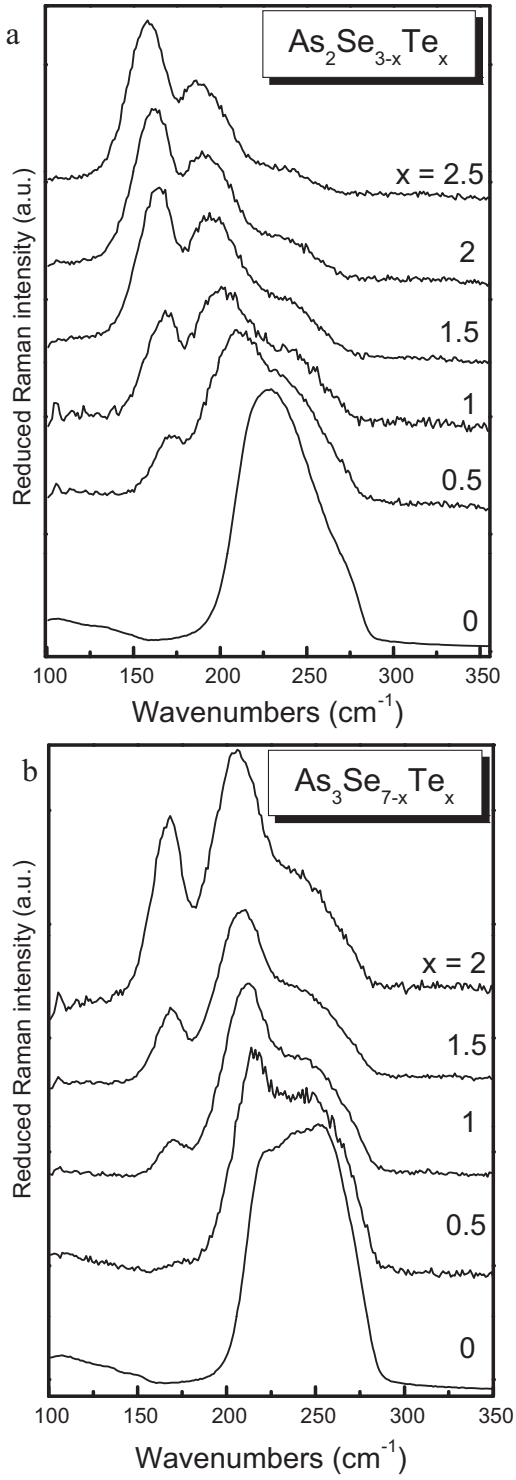

Fig. 3. Raman spectra of bulk glasses $As_2Se_{3-x}Te_x$ (a) and $As_3Se_{7-x}Te_x$ (b).

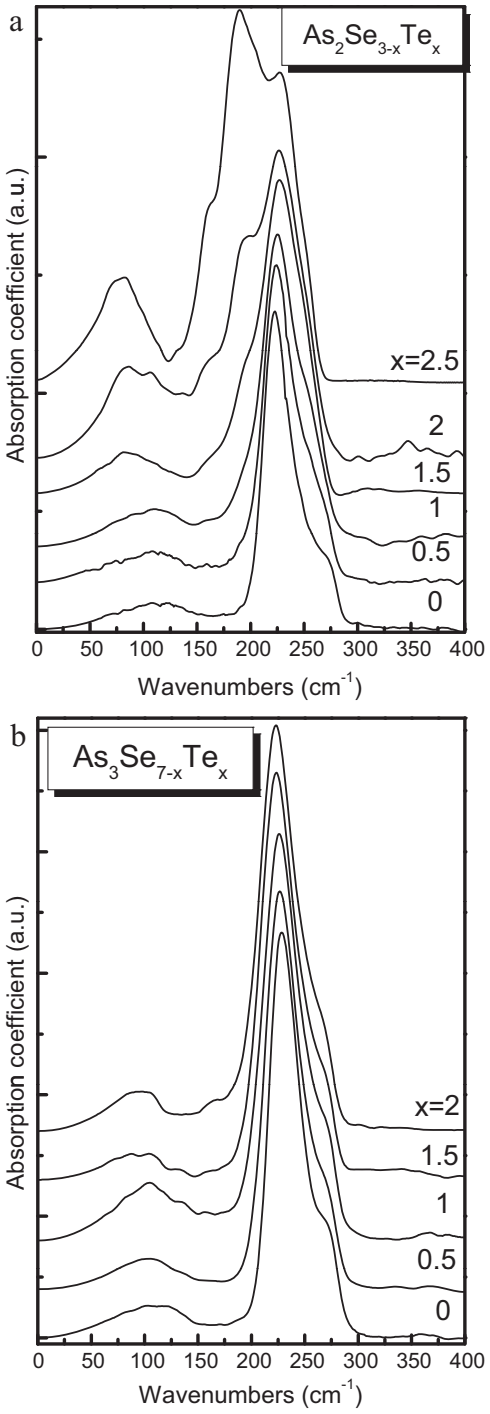

Fig. 4. Far-infrared spectra bulk glasses $As_2Se_{3-x}Te_x$ (a) and $As_3Se_{7-x}Te_x$ (b).

structure, a WAXS experiment was made first on a pristine 400 μm in diameter fiber of $As_3Se_5Te_2$ glass and then after crushing the same fiber into powder (Fig. 7). The major difference in the measured RDFs concerns the amplitude of the peak at 0.17 nm, with no significant changes being observed in the position of other features with the exception of a very small peak at 0.31 nm in the Se, $As_3Se_{6.5}Te_{0.5}$ and As_2Se_3 compositions (Figs. 5 and 6) likely related to a small amount of As and/or Se atoms bridged by oxygen atoms.

The first neighbor peak of the RDF of vitreous Se, glassy $As_3Se_{7-x}Te_x$ ($0 \le x \le 3$) and glassy $As_2Se_{3-x}Te_x$ ($0 \le x \le 2.5$) systems is located at a distance $r_1 = 0.24$ nm (Figs. 5 and 6), which correspond to Se–Se bond and/or Se–As bonding. By increasing the amount of tellurium in glass, this peak shifts slightly to higher r value (from $r_1 = 0.24$ nm to $r_1' = 0.26$ nm). This result is consistent with the formation of As–Te or Se–Te bonds. Therefore, the formation of Te–Te bonds is unlikely even in the tellurium richest glass composition, at least in amounts sufficient to influence the average bonding since feature is observed at ca. $r = 0.28$ nm. The second peak at ca. $r_2 = 0.36$ nm observed for all compositions corresponding to Se/Se, Se/As and Te correlations. This distance is governed by the bond

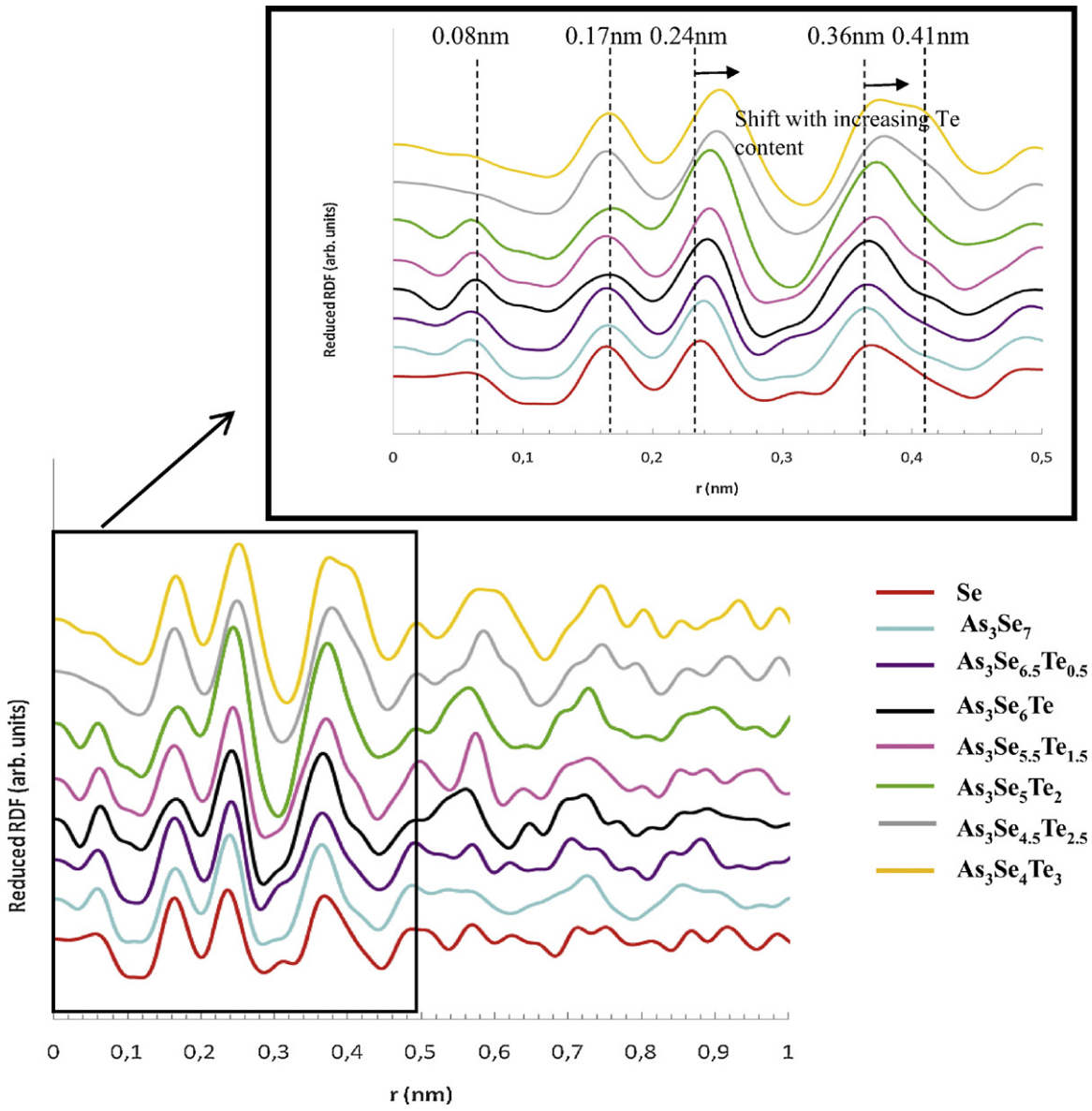

Fig. 5. Comparison of experimental RDFs for vitreous Se and $As_3Se_{7-x}Te_x$ ($0 \le x \le 3$) glasses.

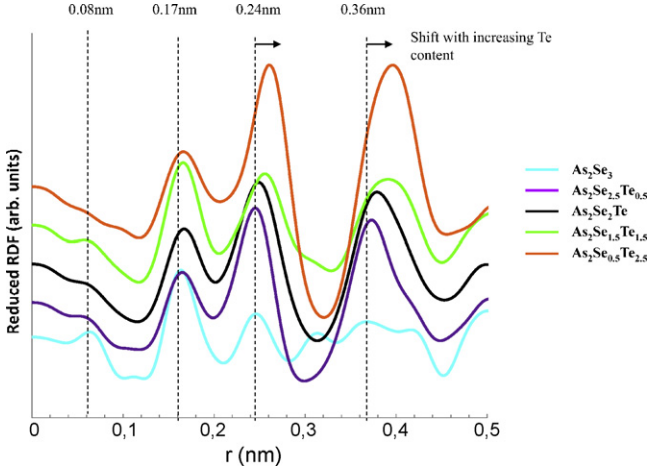

Fig. 6. Experimental RDFs of glasses $As_2Se_{3-x}Te_x$ ($0 \le x \le 2.5$).

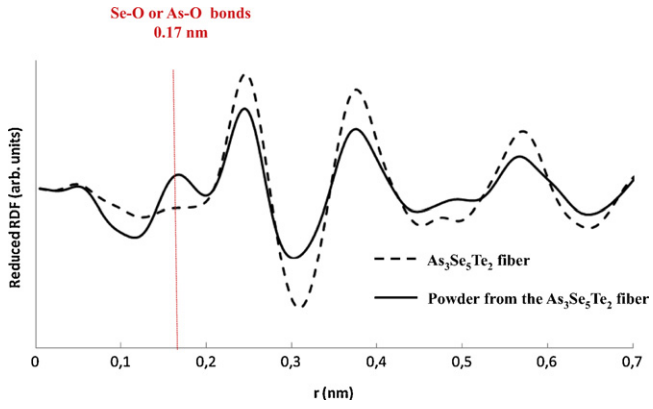

Fig. 7. Comparison of the experimental RDFs of a 400 μm in diameter fiber of glass $As_3Se_5Te_2$ before and after crushing the fiber into powder.

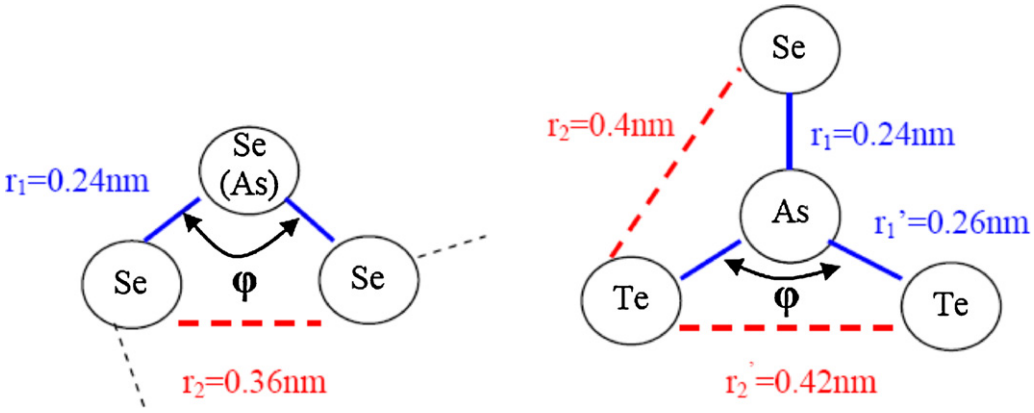

Fig. 8. Schematic bonding configurations for the first-neighbor distance (r_1) and the second-neighbor distance (r_2) in vitreous Se, $As_3Se_{7-x}Te_x$ and $As_2Se_{3-x}Te_x$ glasses.

angle φ shown schematically in Fig. 8, and shows a clear composition dependence. In particular, the peak at ca. r_2 = 0.36 nm becomes broader and develops a second maximum around 0.41 nm as the tellurium content increases. Assuming a bond angle of $\varphi = 109^\circ$, different bonding configurations are possible for the second-neighbor distance according to the WAXS results and include $As(Se_2Te)$ and $As(SeTe_2)$ pyramidal units (Fig. 8).

4. Conclusions

The combined results of infrared, Raman, ^{77}Se NMR and WAXS measurements on $As_3Se_{7-x}Te_x$ ($0 \le x \le 3$) and $As_2Se_{3-x}Te_x$ ($0 \le x \le 2.5$) glasses allows for a better understanding of the structure of these chalcogenide glassy materials. As the tellurium content increases in these ternary glass systems, it was found that:

I. First-neighbor Te–Te bonds are unlikely to form. Tellurium enters the glass network homogeneously by destructing Se short-chain sequences.
II. Mixed pyramidal units $AsSe_{3-x}Te_x$ are formed. At low tellurium contents [$AsSe_2Te$] entities are most favorable, while at higher contents Te–Te second-neighbors exist in [$AsTe_2Se$] entities.

These results are in good agreement with a previous work on the $As_3Se_5Te_2$ glass composition, by reverse Monte Carlo from X-ray data, neutron scattering and EXAFS techniques [8]. The structural model proposed in [8] is totally compatible with the conclusions of the present work. In addition, the absence of Te–Te bonding in As–Se–Te glasses appears to be the origin of their good glass-forming ability, thermal stability and resistivity against crystallization, since Te–Te bonding act usually as a good nucleating agent.

The present findings regarding the nature of chemical bonding are also consistent with the progressive shift of infrared absorption to longer wavelengths as selenium is substituted by the heavier tellurium. This extension of the transmission window in the far-infrared spectral domain suggest the use of As–Se–Te rather than As–Se glasses for the development of optical fiber sensors [4–6].

Acknowledgment

Partial support of this work by the EU is gratefully acknowledged (Marie Curie Actions–NANONLO project, grant MTKD-CT-2006-042301).

References

[1] Z.U. Borisova, Glassy Semiconductors, Plenum Press, New York, 1981.
[2] A.R. Hilton, Proc. SPIE Infrared Fiber Opt. III, vol. 1591, 1991, pp. 34–42.
[3] N.J. Pitt, G.S. Sapsford, T.V. Clapp, R. Worthington, M.G. Scott, Proc. SPIE Int. Soc. Opt. Eng., vol. 618, 2nd ed., 1986, p. 124.
[4] S. Maurugeon, S.B. Bureau, B.C. Boussard-Pledel, A. Faber, X. Zhang, W. Geliesen, J. Lucas, J. Non-Cryst. Solids 355 (2009) 2074–2078.
[5] G. Delaizir, J.-C. Sangleboeuf, E.A. King, Y. Gueguen, X.-H. Zhang, C. Boussard-Pledel, B. Bureau, P. Lucas, J. Phys. D: Appl. Phys. 42 (2009) 095405.
[6] N.A. Hegab, M.A. Afifi, H.E. Atyia, A.S. Farid, J. Alloys Compd. 477 (2009) 925–930.
[7] P. Lucas, M.A. Solis, D. Lecoq, C. Junker, M.R. Riley, J. Collier, D.E. Boesewetter, C. Boussard, B. Bureau, Sens. Actuators, B 119 (2006) 355–362.
[8] D. Le Coq, K. Michel, J. Keirsse, C. Boussard-Plédel, G. Fonteneau, B. Bureau, J.M. Le Quéré, O. Sire, J. Lucas, C. R. Chim. 5 (2002) 907–913.
[9] P. Houizot, C. Boussard-Pledel, A.J. Faber, L. Cheng, B. Bureau, P.A. Nijnatten, W. Gielesen, J. Pereira, J. Lucas, Opt. Exp. 15 (2007) 12529–12538.
[10] H.L. Ma, X.H. Zhang, J. Lucas, H. Senapati, R. Böhmer, C.A. Angell, J. Sol. State Chem. 96 (1992) 181–191.
[11] P. Jovari, B. Bureau, I. Kaban, V. Nazabal, B. Beuneu, U. Rutt, J. Alloys Compd. 488 (2009) 39–43.
[12] P. Lucas, E.A. King, O. Gulbiten, J.L. Yarguer, E. Soignard, B. Bureau, Phys. Rev. B 80 (2009) 214114.
[13] E.L. Gjersing, S. Sen, B.G. Aitken, J. Phys. Chem. C 114 (2010) 8601–8608.
[14] S. Sen, E.L. Gjersing, B.G. Aitken, J. Non-Cryst. Solids 356 (2010) 2083–2088.
[15] E.I. Kamitsos, Phys. Rev. B 53 (1996) 14659–14662.
[16] E.I. Kamitsos, Y.D. Yiannopoulos, C.P. Varsamis, H. Jain, J. Non-Cryst. Solids 222 (1997) 59–68.
[17] F. Dassenoy, M.-J. Casanove, P. Lecante, C. Pan, K. Philippot, C. Amiens, B. Chaudret, Phys. Rev. B 63 (2001), 235407/1–235407/7.
[18] B. Bureau, J. Troles, M. LeFloch, F. Smektala, G. Silly, J. Lucas, Solid State Sci. 5 (2003) 219–224.
[19] R. Golovchak, O. Shpotyuk, A. Kozdras, M. Vicek, B. Bureau, A. Kovalskiy, H. Jain, J. Phys.: Condens. Matter 20 (2008), 245101/1–245101/7.
[20] R. Glovchak, O. Shpotyuk, A. Kozdras, B. Bureau, M. Vlcek, A. Ganjoo, H. Jain, Philos. Mag. (2007) 4323–4334.
[21] B. Bureau, C. Boussard-Pledel, M. LeFloch, J. Troles, F. Smektala, J. Lucas, J. Phys. Chem. 109 (2005) 6130–6135.
[22] G. Lucovsky, Phys. Rev. B 6 (1972) 1480–1489.
[23] G. Lucovsky, R.M. Martin, J. Non-Cryst. Solids 8–10 (1972) 185–190.
[24] G. Lucovsky, A. Mooradia, W. Taylor, G.B. Wright, R.C. Keezer, Solid State Commun. 5 (1967) 113–117.
[25] T. Ohsaka, J. Non-Cryst. Solids 17 (1975) 121–128.
[26] T. Mori, S. Onari, T. Arai, J. Appl. Phys. 19 (1980) 1027–1031.
[27] M.S. Iovu, E.I. Kamitsos, C.P.E. Varsamis, P. Boolchand, M. Popescu, J. Optoelectron. Adv. Mater. 7 (2005) 1217–1221.
[28] A. Mendoza-Galvan, E. Garcia-Garcia, Y.V. Vorobiev, J. Gonzalez-Hernandez, Microelectron. Eng. 51–52 (2000) 677–687.
[29] V.Q. Nguyen, J.S. Sanghera, J.A. Freitas, I.D. Aggarwal, I.K. Lloyd, J. Non-Cryst. Solids 248 (1999) 103–114.
[30] J. Hu, X. Sun, A.M. Agarwal, J.F. Viens, L.C. Kimerling, L. Petit, N. Carlie, K.C. Richardson, T. Anderson, J. Choi, M. Richardson, J. Appl. Phys. 101 (2007) 063520.